

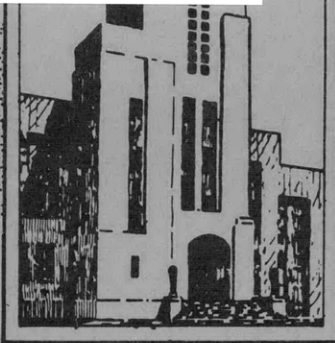
V393
.R46

#1

MIT LIBRARIES



3 9080 02754 3393



DEPARTMENT OF THE NAVY
DAVID TAYLOR MODEL BASIN

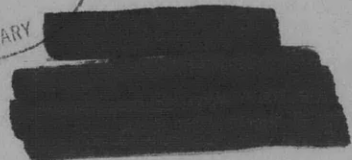
HYDROMECHANICS

LAMINAR SEPARATION OF FLOW AROUND SYMMETRICAL
STRUTS AT VARIOUS ANGLES OF ATTACK

by

AERODYNAMICS

P.K. Chang and W.H. Dunham



STRUCTURAL
MECHANICS

HYDROMECHANICS LABORATORY
RESEARCH AND DEVELOPMENT REPORT

APPLIED
MATHEMATICS

January 1961

Report 1365

1000

**LAMINAR SEPARATION OF FLOW AROUND SYMMETRICAL
STRUTS AT VARIOUS ANGLES OF ATTACK**

by

P.K. Chang and W.H. Dunham

January 1961

**Report 1365
S-R009 01 01**

TABLE OF CONTENTS

	Page
ABSTRACT	1
INTRODUCTION	1
EXPERIMENTS	2
Test Facilities and Apparatus	2
Test Procedure	4
Test Results	6
ANALYSIS	11
DISCUSSION	15
CONCLUSIONS	15
ACKNOWLEDGMENT	15
APPENDIX	16
REFERENCES	20

LIST OF FIGURES

	Page
Figure 1 – Low Turbulence Wind Tunnel	2
Figure 2 – Method of Introducing Dust into the Separated Region of Flow	3
Figure 3 – Cylindrical Model	3
Figure 4 – Group I Strut	4
Figure 5 – Group II Strut	4
Figure 6 – Laminar Separation of Flow-Group I Strut	5
Figure 7 – Laminar Separation of Flow-Group II Strut	6
Figure 8 – Measurements of Laminar Separation Points of Group I Struts (Lower Surface)	9
Figure 9 – Measurements of Laminar Separation Points of Group I Struts (Upper Surface)	9
Figure 10 – Laminar Separation Points on the Lower Surface of Group II Struts as a Function of Angle of Attack	10
Figure 11 – Potential Velocity Distribution of Group II Strut at Angles of Attack	12
Figure 12 – Coordinate System for Computation of Separation Points for Group II Strut	14

LIST OF TABLES

Table 1 – Experimental Values of Laminar Separation Point for a Group I Strut with Chord Length of 4 Inches	7
Table 2 – Experimental Values of Laminar Separation Point for a Group I Strut with Chord Length of 6 Inches	8
Table 3 – Experimental Values of Laminar Separation Point for a Group II Strut with Chord Length of 9.6 Inches (Lower Surface)	8
Table 4 – Analytical Determination of Laminar Separation Points for Group II Strut, Chord Length of 9.6 Inches (Lower Surface)	14

NOTATION

b	One-half thickness
C_p	Pressure Coefficient
c	Chord length of strut
c_f	Coefficient of friction $c_f = \tau / (1/2 \cdot \rho u_e^2)$
L	One-half of the chord length
m	$m = - (\theta^2 / \nu) (du_e / dx)$
n	Parameter velocity profile $\frac{u}{u_e} = \left(\frac{y}{\delta}\right)^n$
p	Static pressure
Re_c	Reynolds number based upon chord length and undisturbed free-stream velocity
s	Arc length between leading edge and separation point
t	Maximum thickness of Group I strut
t_s	Thickness at laminar separation point of Group I strut
u	Streamwise velocity within the boundary layer
u'	$u' = u_e / u_\infty$
u_e	Streamwise velocity at the edge of boundary layer
u_∞	Undisturbed flow velocity
X	Chordwise coordinate of Group II strut (origin is at the center of strut)
x	Arc length along the surface from the stagnation point
x_0	Value of x where integration begins
x_1	Distance along the surface from the initial point of pressure rise
x_s	Distance measured along the chord from stagnation point to laminar separation point
x'_s	Distance measured along the chord from the leading edge to the point of laminar separation
Y	Axis perpendicular to chord

y	Axis perpendicular to surface
α	Angle of attack
β	$\beta = b/L$
ξ	$\xi = X/L$
ξ'	$\xi = x/L$
η	$\eta = Y/L$
$F(\xi)$	$(1 + \xi) / (1 - \xi)$
δ	Boundary-layer thickness
θ	Boundary-layer momentum thickness
ρ	Density
τ	Shear stress
ϕ	y/δ

ABSTRACT

Laminar separation was determined by the dust method on two symmetrical strut sections with thickness ratios of 50 percent and 9.42 percent. The method consists of dispersing fine dust into the flow near the rear of the strut which had been coated with an oil film. The dust adheres to the strut in the separated regions. If the flow is laminar up to the point of separation, the separated region is clearly delineated. Laminar flow separation points were measured on geometrically similar models within the two groups of struts to determine the effect of Reynolds number and angle of attack. It was determined that the ratio of the distance of separation from the leading edge to the chord length is independent of Reynolds number. As the angle of attack increased, separation shifted forward on the upper surface and aft on the lower surface. On the group of thin struts separation moved to the leading edge on the upper surface at very small positive angles of attack and measurements were confined to the lower surface. The points of laminar separation computed by the analytical methods of Stratford, Shvets, and Thwaites agreed favorably with the experimental values. Therefore, the dust method provides a rapid and accurate experimental technique for locating the region of laminar separation.

INTRODUCTION

The phenomenon of flow separation, in general, is caused by the simultaneous combination of an adverse pressure gradient and a loss in momentum within the inner viscous boundary layer. The flow leaves the body surface at the point of separation which is mathematically defined as a point where the velocity gradient normal to the wall vanishes. If separation can be avoided, large reductions in drag and increases in lift result. The maximum performance of fluid handling devices such as fans, turbines, and compressors, etc. occurs at or near the flow separation. Therefore, a study of laminar separation is important in the design of many aerodynamic and hydrodynamic bodies.

A considerable number of research programs have been carried out on the subject of two-dimensional flow separation. Highly detailed analytical methods, as well as approximate calculations, have been successful in determining the laminar separation point. However, experimentation has been difficult because of the time and expense required for such projects.^{1,4} A simple and rapid experimental method, the so-called "dust method," has been introduced recently by W. Spangenberg of the National Bureau of Standards. It has been used with good results by Smith and Murphy² of the Douglas Aircraft Co. for the study of separation on bodies of revolution. This method consists of dispersing talcum dust in the separated

¹References are listed on page 20.

region near the trailing edge of the model. The reverse flow in the separated region carries the dust forward as far as the separation point and it adheres to an oil film painted on the model surface.

A series of experiments, in which the dust method was used, were carried out in the TMB low-turbulence wind tunnel to study laminar separation on struts. Two groups of symmetrical struts were used. Each group contained geometrically similar sections of different chord lengths. The range of angles of attack for the experiment was from 0 to 45 degrees. The positions of the separation point were determined by measuring the length of the white powder deposit left after each run.

The experimental results were compared with three analytical methods: those by Stratford, Shvets, and Thwaites.

EXPERIMENTS

TEST FACILITIES AND APPARATUS

The experiments were carried out in the TMB Eiffel-type,³ low-turbulence wind tunnel (Figure 1). It has a rectangular test section 2 ft wide, 4 ft high, and 15 ft long. The intake air of the tunnel is supplied by a room (67 ft × 135 ft × 45 ft) which is, in effect, a settling reservoir. The turbulence level of about 0.1 percent is achieved by using six turbulence damping screens and by a contraction ratio of 12.5: 1. The dust dispenser used in the dust

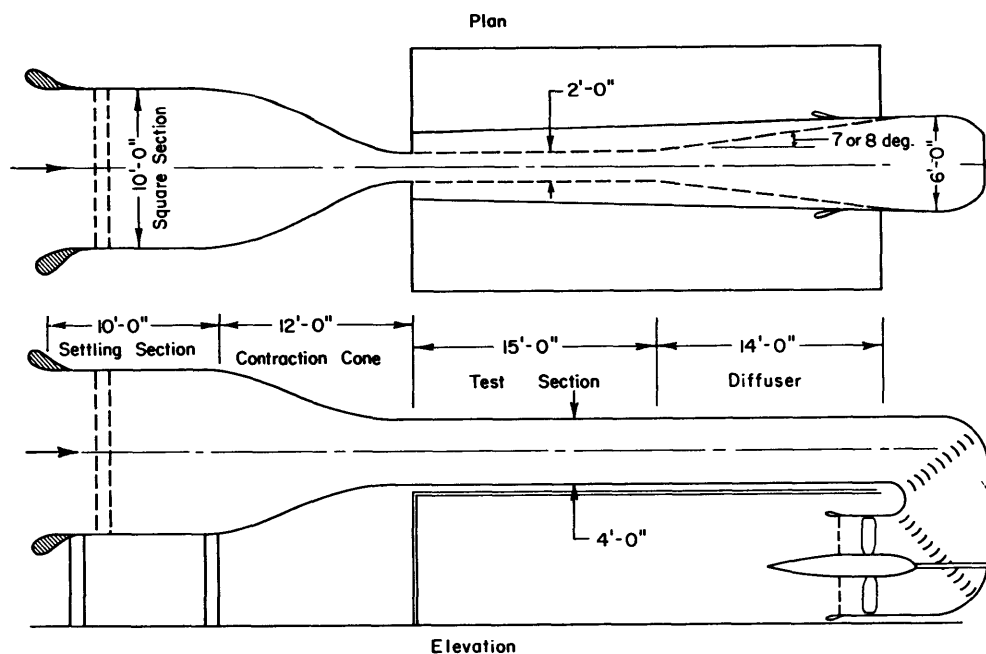


Figure 1 – Low-Turbulence Wind Tunnel

method consisted of a metal container filled with talcum powder. An air supply pressure of 35 psi was used to distribute the dust in the vicinity of the trailing edge of the model through the tubing shown in Figure 2.

The models used in the experiment consist of three basic shapes: a cylinder (Figure 3) and two groups of thick and thin symmetrical struts (Figure 4 and 5 respectively). The thick struts, hereafter called Group I struts, have a 50 percent thickness ratio and chord length of 2, 4, 6, 8, and 10 inches. The thin struts (Group II) have a 9.42 percent thickness ratio, and chord lengths of 9.6 and 19.2 inches. The strut section is given by the intersection of two circular arcs.

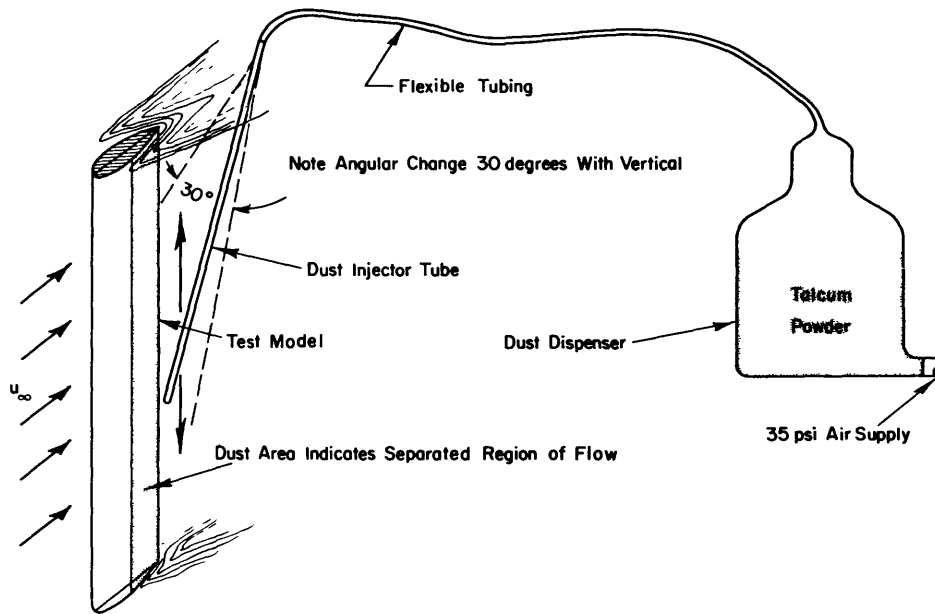


Figure 2 – Method of Introducing Dust into the Separated Region of Flow

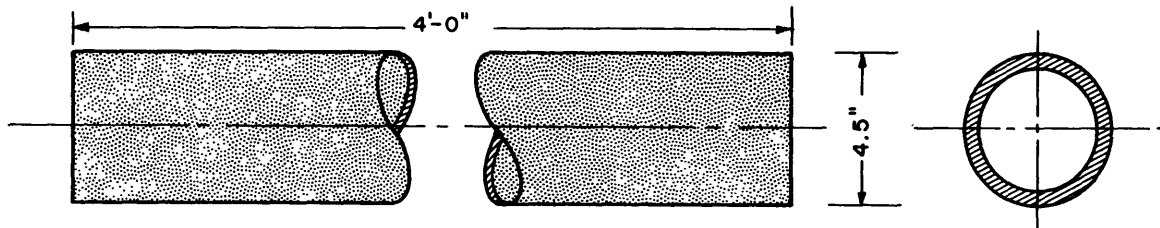
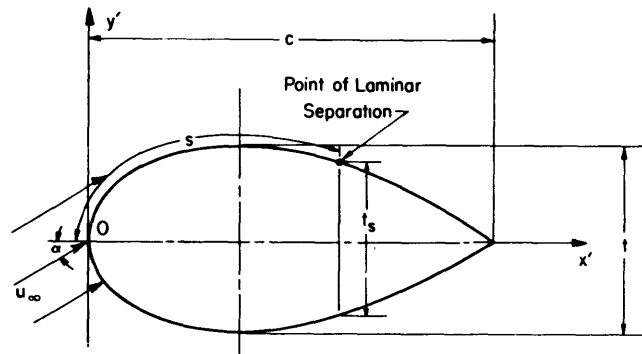


Figure 3 – Cylindrical Model



Nose Radii = $0.57532 \frac{t^2}{c}$, $\frac{t}{c} = 0.5$

$a = 0.4361302$

$b = 0.3083906$

$c = \text{Chord}$

$t = \text{Maximum Thickness}$

$0 \leq \frac{x'}{c} < 0.436$

$0.436 \leq \frac{x'}{c} \leq 0.872$

$0.872 \leq \frac{x'}{c} \leq 1.0$

$$y' = \frac{t}{2} \left\{ 1 - \left[\frac{1}{a} \left(a - \frac{x'}{c} \right)^2 \right] \right\}^{\frac{1}{2}}$$

$$y' = \frac{t}{2} \left\{ \left\{ 1 - \left[\frac{1}{2} \left\{ \frac{1}{a} \left(\frac{x'}{c} - a \right) \right\}^2 \right] \right\} \right\}$$

$$y' = \frac{t}{4} \left\{ \left[\frac{1}{b} \left(b + 1 - \frac{x'}{c} \right) \right]^2 - 1 \right\}^{\frac{1}{2}}$$

Figure 4 – Group I Strut

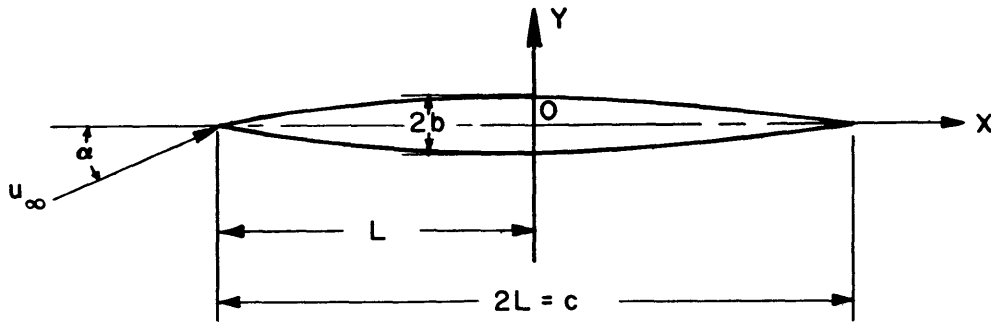


Figure 5 – Group II Strut

TEST PROCEDURE

The models are prepared for testing by applying a thin coat of SAE 10 lubricating oil to the surface of the model. Dust is then injected into the wake of the model near the trailing edge. If separation occurs, the back flow will carry the dust particles forward to the farthest point of separation from the trailing edge, and then away to the free stream. Dust particles will attach to that portion of the oil film, which is in the separation region, leaving a permanent record. There are, however, limitations to this method. Small perturbations in the

position of the point of separation will not be recorded, since the method records only the forward most position of dust.

In order to evaluate the accuracy of this dust method, a smooth aluminum hollow cylinder 4.5 in. diameter and 4 ft long (Figure 3) was mounted vertically inside the wind tunnel. Fine dust was then dispersed uniformly in the wake of the model. A separation angle of 82.5 degrees from the point of stagnation was measured. Niemenz and Kreith,^{4,5} working independently, found that laminar separation occurred between 80 and 85 degrees on a cylinder whose axis was normal to the flow. From this favorable comparison, it is believed the dust method shows sufficient accuracy for the determination of flow separation.

Both groups of symmetrical struts were tested at varying angles of attack and velocities in the Reynolds number region of laminar flow. The models were mounted vertically inside the wind tunnel as shown in Figure 2. Dust was then introduced uniformly into the separated region of flow, by moving the dust injector tube up and down through a hole in the tunnel observation window.

The disturbing influence of the chordwise component of the jet velocity and the presence of the dust in the boundary layer of the separated flow region were evaluated in the following manner: the angular change of the dust jet varies from 30 to 60 degrees with the vertical. This variation in angle causes a change in the chordwise component of the jet velocity by a ratio 1: 1.73. However, the variation in chordwise position of the line of separation was random, and of the order of magnitude of 1 percent. It is therefore concluded that the error introduced by the chordwise component of the velocity of the dust jet is negligible.

The influence of dust on the aerodynamic characteristics of the jet has been studied by Chernov.⁶ The results indicate that dust has little effect when the mass concentration is

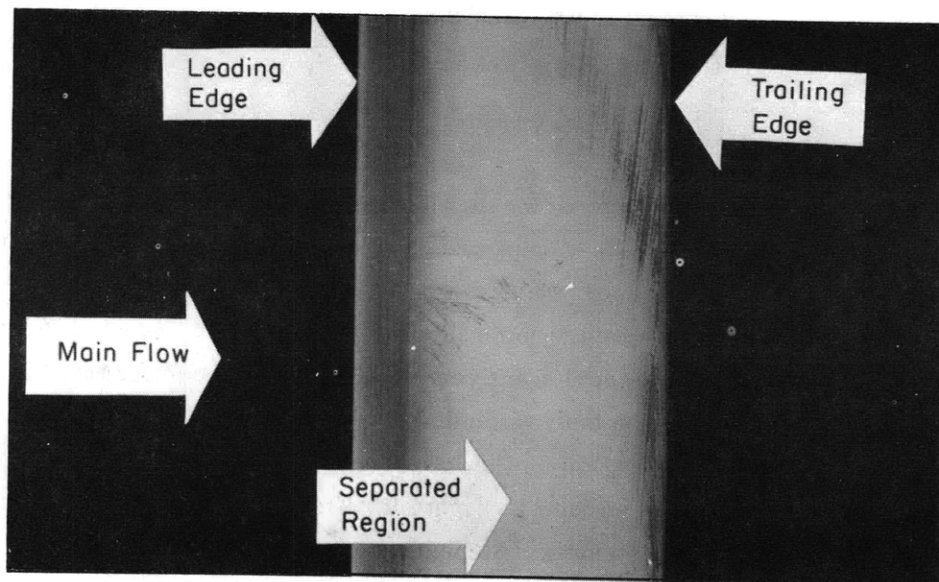


Figure 6 - Laminar Separation of Flow-Group I Strut

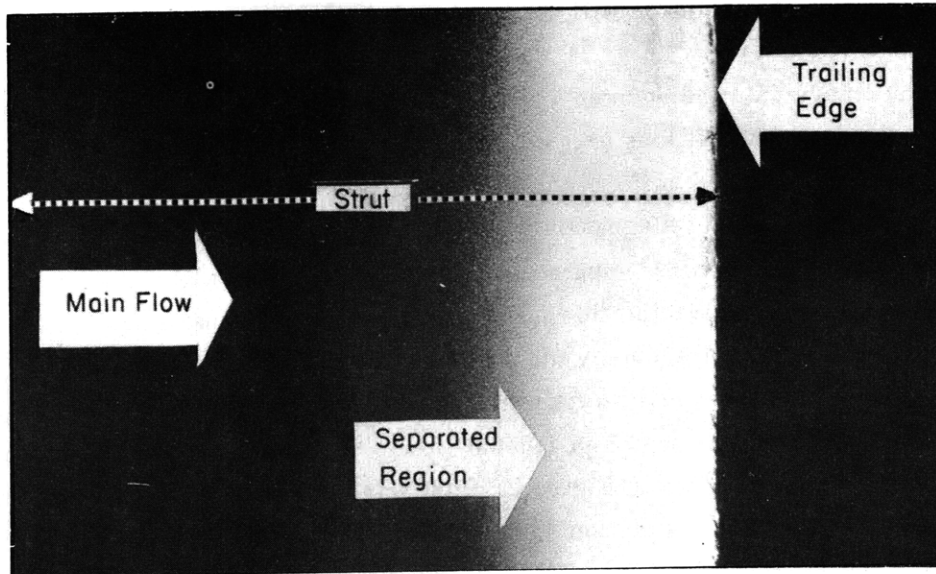


Figure 7 – Laminar Separation of Flow-Group II Strut

A part of the strut is shown at left. Right dark side is wake region.

below 1 lb per lb of air and air jet velocities remain below 97 ft/sec. The mass concentration of dust and the velocities in this experiment are much smaller than the values cited; therefore, the effect of the dust particles is assumed to be negligible.

Photographs of the separated regions of flow on the two groups of struts are shown in Figures 6 and 7. The white areas near the trailing edges are where the dust has adhered and indicates the separated region. Only a portion of the Group II strut is shown in Figure 7; the black area on the left is the unseparated flow on the strut, the white area is the separated region and the black area on the right is the wake region.

TEST RESULTS

The laminar separation points were located by measuring the distances from the leading edge along the surface to the point of separation. The measured values of s for two Group I struts are given in Tables 1 and 2 and are plotted in Figures 8 and 9. Each point represents the average of several measurements in a range of Reynolds numbers from 9.4×10^3 to 2.09×10^5 . Values for the 4-in. chord are given in Table 1 and those for the 6-in. chord in Table 2. The flow was laminar on both surfaces over quite a range of angles of attack. Measured locations of laminar separation on the lower surface of Group I struts are plotted in Figure 8 and those for the upper surface in Figure 9. From these two figures it can be seen that the point of laminar separation is independent of Reynolds numbers.

The measurements of laminar separation of the Group II struts in the range of free stream Reynolds numbers, $Re_c = 1.6 \cdot 10^4$ to $1.02 \cdot 10^5$, at varying angles of attack are

shown in Table 3. At zero angle of attack, the flow around the strut was symmetrical and laminar, and the flow separated on both the upper and lower surfaces. But, at other angles of attack, the flow on the upper surface of the Group II struts became turbulent because of the sharp leading edge and the very large adverse pressure gradient. The lower surface, however, remained in the laminar flow region. The point of separation was determined by the dust method on the lower surface in a range of Reynolds numbers, based upon the undisturbed free stream velocity and chord length, from $1.27 \cdot 10^5$ to $1.5 \cdot 10^5$. Angles of attack from zero to 45 degrees were used and the measured values of x'_s , the chordwise distance from the leading edge to separation, are shown in Table 3 and Figure 10.

TABLE 1
Experimental Values of Laminar Separation Point for a
Group I Strut with Chord Length of 4 Inches

Angle of Attack (degrees)	Distance Along Surface of Laminar Separation Point from the Leading Edge (s) (inches)	Distance of Laminar Separation Point from Leading Edge/ Chord Length (s/c)
(a) Lower Surface	$(Re_c = 0.94 \cdot 10^5 \text{ to } 1.42 \cdot 10^5)$	
0	2.04	0.51
5	2.38	0.59
10	2.56	0.64
15	2.89	0.72
30	3.65	0.91
45	4.00	1.0
(b) Upper Surface	$(Re_c = 1.2 \cdot 10^5)$	
0	2.04	0.51
5	1.69	0.36
10	1.44	0.30
15	1.31	0.28
30	0.69	0.14

TABLE 2

Experimental Values of Laminar Separation Point for a Group I Strut with Chord Length of 6 Inches

Angle of Attack (degrees)	Distance Along Surface of Laminar Separation Point from the Leading Edge (s) (inches)	Distance of Laminar Separation Point from Leading Edge/ Chord Length (s/c)
(a) Lower Surface	$(Re_c = 1.4 \cdot 10^5 \text{ to } 2.09 \cdot 10^5)$	
0	3.08	0.51
5	3.57	0.59
10	4.11	0.69
15	4.29	0.72
30	5.86	0.98
45	6.28	1.05
(b) Upper Surface	$(Re_c = 1.8 \cdot 10^5)$	
0	3.08	0.51
5	2.46	0.34
10	2.19	0.31
15	1.76	0.24
30	0.99	0.14

TABLE 3

Experimental Values of Laminar Separation Point for a Group II Strut with Chord Length of 9.6 Inches (Lower Surface)

$$(Re_c = 1.27 \cdot 10^5 \text{ to } 1.5 \cdot 10^5)$$

Angle of Attack (degrees)	Distance Along Surface of Laminar Separation Point from the Leading Edge (x'_s) (inches)	Distance of Laminar Separation Point from Leading Edge/ Chord Length (x'_s/c)
0	7.5	0.781
5	7.48	0.779
10	8.35	0.870
15	8.50	0.885
20	8.94	0.931
30	9.19	0.957
45	9.32	0.971

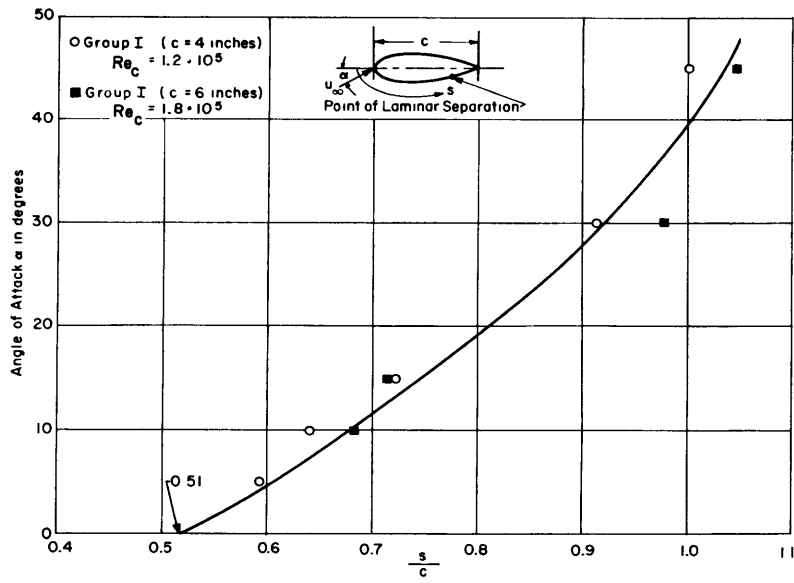


Figure 8 – Measurements of Laminar Separation Points of Group I Struts (Lower Surface)

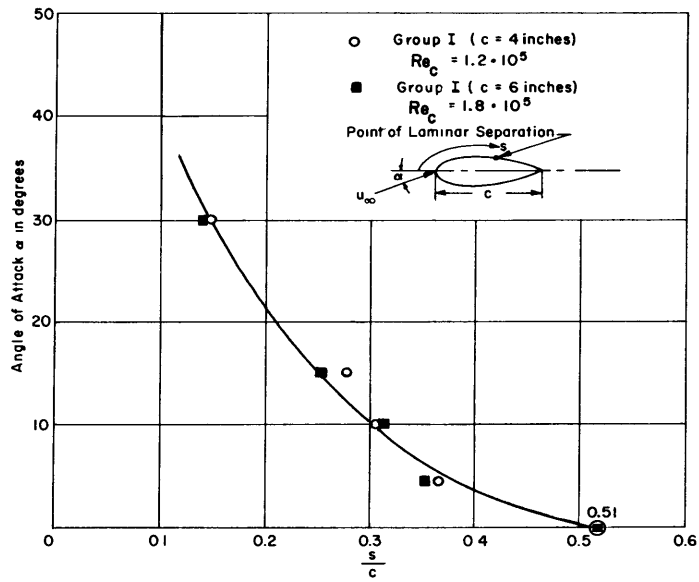


Figure 9 – Measurements of Laminar Separation Points of Group I Struts (Upper Surface)

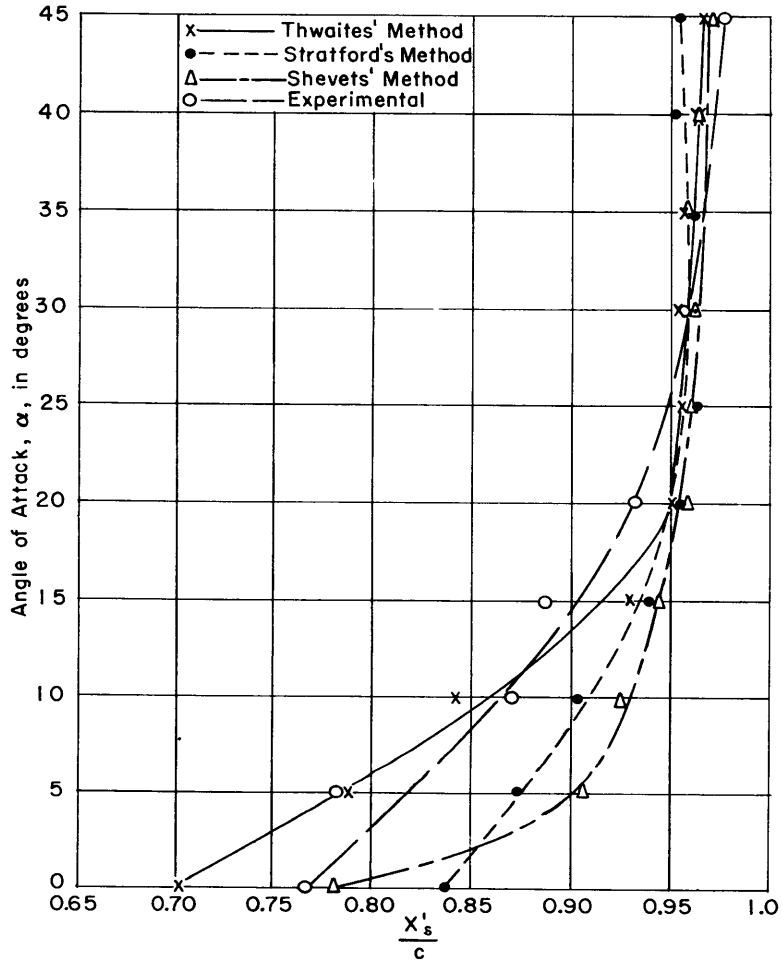


Figure 10 – Laminar Separation Points in the Lower Surface of Group II Struts as a Function of Angle of Attack

In Table 3 the numerical values of x'_s are average values of several test runs. The free stream velocities were between 25 and 30 ft/sec. The test results show that values of x'_s / c for this group of struts as well as those in Group I are not affected by free-stream velocities or Reynolds numbers.

Computations of wall effects for both groups of struts indicate that correction for the angle of attack would be negligible.

ANALYSIS

The experimental data obtained are compared with analytical results. For the analysis it is necessary to determine the potential velocity distribution over the strut. As the Group I struts have a thick cross section and a complicated geometry it is not easy to obtain the potential velocity distribution. But as the Group II struts are thinner and have biconvex sections, the potential velocity distribution may be computed. Therefore, the analysis will be made for struts in the Group II class.

The Group II strut section is the intersection of two circular arcs. Referring to Figure 5.

$$Y(X) = \pm b \left[1 - \left(\frac{X}{L} \right)^2 \right] \quad [1]$$

where the origin of the coordinate system is at the center of the strut and $2L$ is the chord length. The upper sign refers to the upper surface of the strut and the lower sign to the lower surface. In dimensionless form, Equation [1] may be written as

$$\eta = \pm \beta [1 - \xi^2] \quad [2]$$

where $\eta = \frac{Y}{L}$, $\xi = \frac{X}{L}$, and $\beta = \frac{b}{L}$

The potential flow velocity distribution about this biconvex strut configuration based upon the coordinates X and Y is given by Van Dyke⁷ as follows:

$$u' = 1 + \left(\frac{2}{\pi} \right) \beta \left\{ 2 - \xi \ln F(\xi) \right\} + (\beta)^2 \left[\frac{3}{\pi^2} \left\{ 2 - \xi \cdot F(\xi) \right\}^2 - \frac{1}{\pi^2} \ln^2 F(\xi) - (1 - \xi)^2 \right] \pm \alpha F(\xi)^{-1/2} \mp \frac{\alpha}{\pi} \beta F(\xi)^{-1/2} [(1 + 2\xi) \ln F(\xi) - 4] - \frac{1}{2} \alpha^2 \quad [3]$$

where

$$F(\xi) = \frac{(1 + \xi)}{(1 - \xi)}, \quad u' = \frac{u_e}{u_\infty},$$

and α is angle of attack. Upper signs indicate the potential flow distribution on the upper surface and the lower signs on the lower surface.

The velocity distribution of Equation [3] is plotted in Figure 11. As the angle of attack decreases the stagnation point on the lower surface shifts forward and reaches the leading edge at zero angle of attack. At nonzero angles of attack the flow divides at the stagnation point. Part of it flows in the forward direction, turns around the leading edge, and becomes turbulent on the upper surface due to the very large adverse pressure gradient. The flow aft of the stagnation point is toward the rear and is laminar up to the point of separation. At zero angle of attack the flow is symmetrical and is laminar on both surfaces of the strut at the Reynolds numbers investigated. At the leading edge a mathematical singularity in velocity occurs because $\ln F(\xi)$ is negatively infinite. At angles of attack other than zero the singularity does not influence numerical computations because the region of interest on the lower surface lies aft of the stagnation point which is downstream of the leading edge. At zero angle of attack the leading edge is the stagnation point and the computed curve is modified to pass through zero.

The experimental results obtained on the Group II struts will now be compared with three analytical methods, those by Stratford, Shvets, and Thwaites. A brief description of these methods, the coordinate system used, and the results of the calculations are given in the following section. A more detailed analysis of these methods is given in the Appendix.

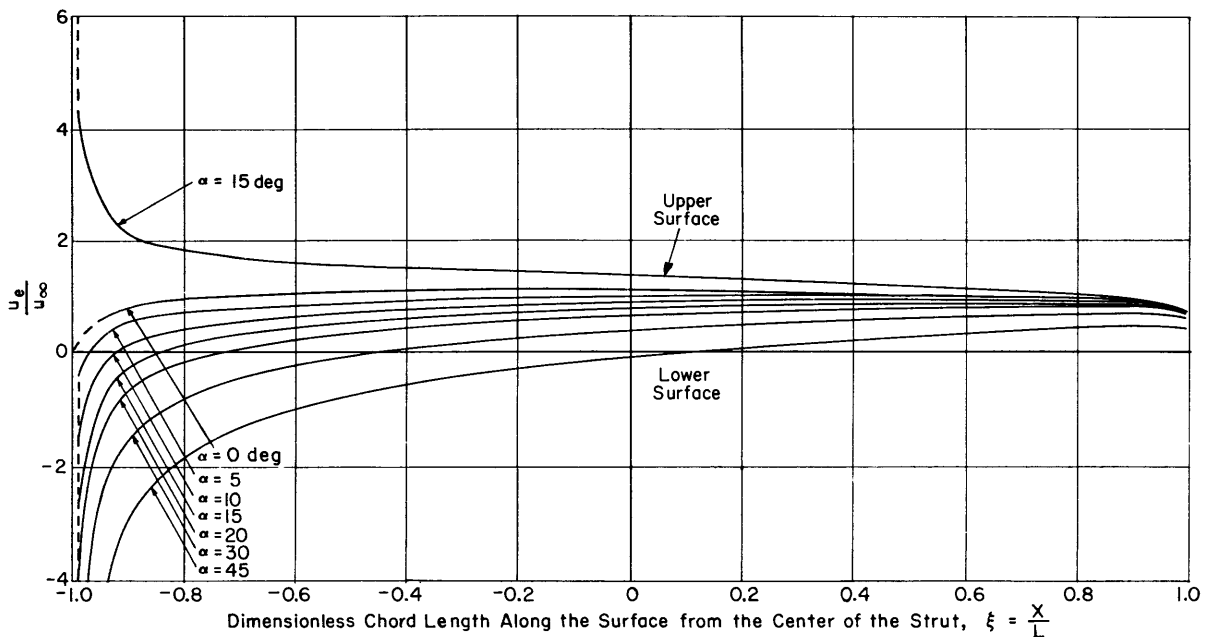


Figure 11 – Potential Velocity Distribution of Group II Strut at Angles of Attack

MODIFIED STRATFORD CRITERION^{8,9}

The modified Stratford method is simple and the criterion of separation is given by terms of the potential flow pressure coefficient. The modified Stratford criterion may be expressed as

$$x_1^2 C_p \left(\frac{dC_p}{dx_1} \right)^2 = 0.0104$$

where x_1 is the distance measured on the lower surface from the initial point of pressure rise to the point of laminar separation. In the Group II models, x_1 is measured aft of the point of maximum potential velocity in the laminar flow region. Since

$$C_p = 1 - \left(\frac{u_e}{u_{\max}} \right)^2$$

then

$$\frac{dC_p}{dx_1} = -2 \frac{\frac{u_e}{u_{\max}} \left\{ d \left(\frac{u_e}{u_{\max}} \right) \right\}}{dx_1}$$

SHVETS CRITERION¹⁰

The Shvets method of prediction is the result of a second-order approximation to the solution of boundary-layer equation. This solution is then evaluated at the boundary condition of $\left(\frac{\partial u}{\partial y} \right)_{\text{wall}} = 0$. The Shvets criterion is again expressed by terms of potential flow only. Laminar separation occurs if the following relation is satisfied.

$$4 \left(\frac{du'}{d\xi'} \right) (u')^{-6} \int_0^{\xi'} \{ u'(\xi') \}^5 d\xi' = -1$$

where $u' = \left(\frac{u_e}{u_\infty} \right)$ and $\xi' = \left(\frac{x}{L} \right)$. Here x is measured aft of the stagnation point along the strut surface and y is the outward normal to the surface. Due to the small thickness ratio the arc length along the strut surface may be approximated by a straight line parallel to the chord.

THWAITES CRITERION¹¹

Thwaites criterion contains terms of viscosity and boundary layer, in addition to the potential velocity gradient. Therefore, more elaborate calculation is needed for its evaluation

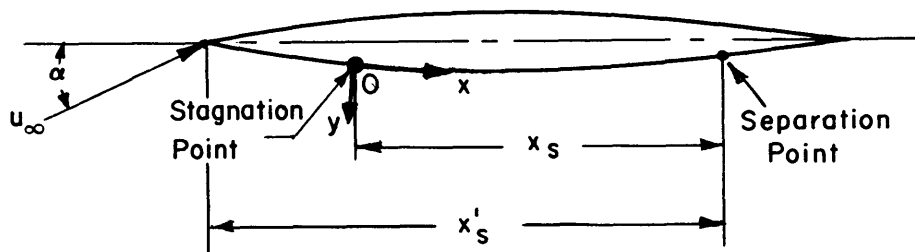


Figure 12 – Coordinate System for Computation of Separation Points for Group II Strut

than in Stratford and Shvets methods. Thwaites method was modified by Curle and Skan¹² and its criterion for the laminar separation is given by

$$m = - \left(\frac{\theta^2}{\nu} \right) \left(\frac{d u_e}{dx} \right) = 0.090$$

where θ is momentum thickness of boundary layer and may be computed by Truckenbrodt's method.¹³ The values of x and y are defined in Figure 12.

The predicted positions of laminar separation at various angles of attack by the above three methods are summarized in Table 4 and shown graphically in Figure 10.

TABLE 4

Analytical Determination of Laminar Separation Points for Group II Strut, Chord Length of 9.6 Inches (Lower Surface)

Angle of Attack (degrees)	Distance from the Leading Edge to the Point of Laminar Separation per Chord Length (x'_s/c)		
	Thwaites' Method	Shvets' Method	Stratford's Method
0	0.7037	0.777	0.8346
5	0.791	0.907	0.875
10	0.84	0.9225	0.905
15	0.93	0.945	0.9425
20	0.951	0.955	0.955
25	0.954	0.962	0.962
30	0.954	0.959	0.958
35	0.955	0.956	0.954
40	0.963	0.963	0.952
45	0.973	0.973	0.954

DISCUSSION

Figure 10 gives a comparison of the analytical results and the experimental data. At lower angles of attack the agreement among the predicted positions with experimental data is obtained closely by Thwaites method. Only at zero angle of attack does Shvets method give the best prediction among the three methods. In the region of higher angles of attack, the agreement between experiment and analysis improves. The reason for this discrepancy among the analytical results may be explained by Schlichting's⁴ analysis of the position of separation. Schlichting points out that laminar separation can be calculated only approximately when the point of separation is situated comparatively far behind the point of minimum pressure. The position of the minimum pressure of potential flow of Group II struts is located at the midchord of zero angle of attack. With increase of angle of attack the positions of the minimum pressure and of the laminar separation shift toward the trailing edge. However, the displacement of the position of minimum pressure is larger than the displacement of separation as the angles of attack increase. Hence, at lower angles of attack, the distance between the positions of minimum pressure and separation is comparatively larger than at higher angles of attack. Thus, the analytical results can be expected to yield only approximate locations of the laminar separation at the smaller angles of attack.

CONCLUSIONS

From the experiments with the dust method and comparisons with analyses at various angles of attack in two-dimensional flow, the following conclusions are made:

1. The dust method is a rapid and accurate experimental method for the determination of the laminar flow separation on bodies of arbitrary shape.
2. Experiments of symmetrical and geometrically similar struts show that the point of laminar separation, as percent of chord, is independent of Reynolds number within the laminar region, and is dependent only on the geometric configuration of the section.
3. Good agreement was obtained between the analytical results and the experimental data for the location of the laminar separation point for both symmetrical and asymmetrical laminar flow over the strut surfaces.

ACKNOWLEDGMENT

The authors wish to express their thanks to Dr. Avis Borden, Dr. M.C. Harrington, and Mr. P.S. Granville for their suggestions and criticism.

APPENDIX

MODIFIED STRATFORD CRITERION

Stratford solved the boundary layer equations for the outer and inner laminar boundary layers. In the inner boundary layer, where viscous forces are more important than inertia forces, there is a balance between the forces produced by the pressure gradient and by viscous effects. In the outer layer, where viscous forces are small, there is a balance between inertia forces and those produced by the pressure gradient. Stratford obtained an expression for predicting separation by applying the Blasius boundary layer analysis. Curle and Skan¹² modified Stratford's criterion to give better agreement with Görtler's rigorous solution.¹⁴ The resulting criterion is

$$x_1^2 C_p \left(\frac{dC_p}{dx_1} \right)^2 = 0.0104$$

where x_1 is measured from the initial point of adverse pressure gradient (or aft of the point of maximum potential velocity U_{\max}) and

$$C_p = \frac{p - p_{\min}}{\frac{1}{2} \rho u_{\max}^2}$$

Therefore,

$$\frac{dC_p}{dx_1} = -2 \frac{u_e}{u_{\max}} d \left(\frac{u_e}{u_{\max}} \right)$$

and

$$x_1^2 C_p \left(\frac{dC_p}{dx_1} \right)^2 = 4 \left\{ 1 - \left(\frac{u_e}{u_{\max}} \right)^2 \right\} \xi_1 \left(\frac{du'}{d\xi} \right)^2 \left(\frac{u_e}{u_{\max}} \right)^2 \left(\frac{u_\infty}{u_{\max}} \right)^2$$

where

$$\xi_1 = \frac{x_1'}{L} \text{ and } u' = \frac{u_e}{u_\infty}$$

Since $\frac{u_e}{u_{\max}} = \left(\frac{u_e}{u_\infty} \right) \left(\frac{u_\infty}{u_{\max}} \right)$, values of $\frac{u_e}{u_{\max}}$, $\frac{u_\infty}{u_{\max}}$, $\frac{du_e}{dx_1}$ and $\frac{du'}{d\xi_1}$ were computed at

several locations of x_1 . Then values of x_1 and $x_1^2 C_p \left(\frac{dC_p}{dx_1} \right)^2$ were calculated and a

curve of $x_1^2 C_p \left(\frac{dC_p}{dx_1} \right)^2$ as a function of x_1 was drawn. The point of laminar separation

was determined graphically. The point of laminar separation may be computed more accurately by analytical methods but the labor involved is considerable.

SHVETS CRITERION¹⁰

Shvets formulated his criterion based on the solution of the laminar boundary layer equations to second-order approximations. In physical terms, separation of flow takes place when the shearing stress vanishes at the wall.

The boundary-layer equation with pressure gradient is

$$\frac{\partial^2 u}{\partial y^2} = u \frac{\partial u}{\partial x} - \frac{\partial u}{\partial y} \int_0^y \frac{\partial u}{\partial x} dy - u_e \frac{du_e}{dx}$$

with the boundary conditions

$$u = 0 \quad \text{at } y = 0$$

$$u = u_e \quad y = \delta$$

Solving this equation to a second-order approximation

$$\frac{u}{u_e} = \frac{\delta^2}{24} \frac{du_e}{dx} (\phi^4 - 12\phi^2 - 11\phi) - \frac{\delta}{24} \frac{d\delta}{dx} u_e (\phi^4 - \phi) + \phi$$

where

$$\phi = \frac{y}{\delta}$$

At the edge of the boundary layer $\left. \frac{\partial u}{\partial \phi} \right|_{\phi=1} = 0$

$$\frac{3\delta^2}{8} \frac{du_e}{dx} + \frac{\delta}{8} u_e \frac{d\delta}{dx} = 1$$

Assuming that when $x = 0$, $\delta = 0$, then

$$\delta^2 = \frac{16}{u_e^6} \int_0^x u_e^5 dx$$

The shearing stress at the wall gives

$$\left. \frac{\partial u}{\partial y} \right|_{\text{wall}} = \frac{u_e}{3} \left[\frac{4}{\delta} + \delta \frac{du_e}{dx} \right] = \frac{u_e^4}{3} \left(\int_0^x u_e^5 dx \right)^{-1/2} \left[1 + \frac{4}{u_e^6} \frac{du_e}{dx} \int_0^x u_e^5 dx \right]$$

But at the separation point, $\left. \frac{\partial u}{\partial y} \right|_{y=0} = 0$. This condition is satisfied when

when

$$4 \frac{\frac{du_e}{dx}}{u_e^6} \int_0^x u_e^5 dx = -1$$

In nondimensional form, this equation becomes

$$\left\{ 4 \frac{\left(\frac{du'}{d\xi'} \right)}{(u')^6} \right\} \int_0^{\xi'} \{u'(\xi')\}^5 d\xi' = -1$$

when $\xi' = \frac{x}{L}$.

THWAITES CRITERION¹¹

Thwaites solved the laminar boundary-layer equations and found that there exists a fixed relationship between velocity gradient and boundary-layer thickness, at the position of laminar flow separation. This relation was modified by Curle and Skan¹² to give the following criterion

$$m = -\frac{\theta^2}{\nu} \frac{du_e}{dx} = 0.090$$

The momentum thickness θ is computed using Truckenbrodt's¹³ method.

$$\frac{\theta}{l} = \frac{\left[c_1^* + \left(\frac{c_f}{2} \right)^{1+n} \int_{x_0/l}^{x/l} \left(\frac{u_e}{u_\infty} \right)^{3+2n} d\left(\frac{x}{l} \right) \right]^{\frac{1}{1+n}}}{\left(\frac{u_e}{u_\infty} \right)^3}$$

where l is a characteristic length. Here l is replaced by L . Since the flow is fully laminar from the initial position at $x_0 = 0$, $c_1^* = 0$ and $n = 1$. Furthermore, for laminar flow,

$$\frac{c_f}{2} = \sqrt{0.441} \left(\frac{\nu}{u_\infty x} \right)^{\frac{1}{2}}$$

Hence,

$$\theta^2 = \frac{0.441 \nu x}{u_\infty \left(\frac{u_e}{u_\infty} \right)^6} \int_0^{x/L} \left(\frac{u_e}{u_\infty} \right)^5 d \frac{x}{L}$$

Therefore, the criterion in dimensionless form is

$$m = -0.441 \frac{du'}{d\xi'} (u')^6 \xi' \int_0^{\xi'} (u')^5 d\xi'$$

REFERENCES

1. Gault, I.E., "An Experimental Investigation of Regions of Separated Laminar Flow," National Advisory Committee of Aeronautics, TN 3505 (1955).
2. Smith, A.M.O. and Murphy, J.S., "A Dust Method for Locating the Separation Point," Journal of Aeronautical Science, Vol. 22 (Apr 1955).
3. Wright, E.A., "New Research Facilities at the David Taylor Model Basin," David Taylor Taylor Model Basin Report 1292 (Jan 1959).
4. Schlichting, H. "Theory of Boundary Layer," McGraw-Hill Book Co., New York (1955), pp. 138, 215-216.
5. Kreith, F., "Principles of Heat Transfer," International Text Book Co., Scranton (1958).
6. Chernov, A.D., "The Effect of Solid Admixtures on the Velocity of Motion of a Free Dust Air Jet," National Advisory Committee for Aeronautics, TM 1430 (1957).
7. Van Dyke, M.D., "Second-Order Subsonic Airfoil Theory Including Edge Effects," National Advisory Committee for Aeronautics, Report 1274 (1956).
8. Stratford, B.S., "The Prediction of the Turbulent Boundary Layer," Journal of Fluid Mechanics, Vol. 5 (Jan 1959), p.8.
9. Stratford, B.S., "Flow in the Laminar Boundary Layer Near Separation," Aeronautical Research Council, Technical Report BSM No. 3002 (1957).
10. Shvets, M.E., "Method of Successive Approximations for the Solution of Certain Problems in Aerodynamics," National Advisory Committee for Aeronautics, TM 1268 (1951).
11. Thwaites, B., "Approximate Calculations of the Laminar Boundary Layer," Aeronautical Quarterly, Vol. I (Nov 1949).
12. Curle, N. and Skan, S.W., "Approximate Methods for Predicting Separation Properties of Laminar Boundary Layers," Aeronautical Quarterly, Vol. VIII (Aug 1957).
13. Truckenbrodt, E., "Ein Quadraturverfahren zur Berechnung der Laminaren und Turbulenten Reibungsschicht bei Ebener und Rotationsymmetrischer Strömung," Ingenieur Archiv. II, Bd., Viertes Heft (1952).
- 13a. Truckenbrodt, E., "A Method of Quadrature for Calculation of the Laminar and Turbulent Boundary Layer in Case of Plane and Rotationally Symmetric Flow," National Advisory Committee for Aeronautics, TM 1397 (1955).
14. Görtler, H., "A New Series for the Calculation of Steady Laminar Boundary Layer Flows," Freiburg University Mathematics Institute Report (Sep 1955).

INITIAL DISTRIBUTION

Copies

- 11 CHBUSHIPS
 - 3 Tech Info Br (Code 335)
 - 1 Tech Asst (Code 106)
 - 2 Appl Sci (Code 342)
 - 1 Prelim Des (Code 420)
 - 3 Submarines (Code 525)
 - 1 Propellers Shafting (Code 644)
- 8 CHBUWEPs, Underwater Ord (RUUO)
 - 1 Dr. A. Miller (RR-131)
 - 1 Mr. H.A. Eggers (RUAW-42)
 - 2 Aero & Hydro Br (RAAD-3)
 - 1 Appl Math Br (DCM)
- 4 CHONR
 - 1 Mathematics (Code 432)
 - 2 Mechanics (Code 438)
 - 1 Undersea Programs (Code 466)
- 2 DIR, USNRL
- 4 CDR, USNOL, Mech Div
- 1 CDR, USNOTS, China Lake
- 1 CDR, USNOTS, Pasadena Annex
- 1 NAVSHIPYD MARE
- 1 NAVSHIPYD NORVA
- 2 NAVSHIPYD PTSMH
 - 1 Capt L.A. Rupp
- 1 CDR, USNPG, Dahlgren
- 1 CO & DIR, USNUSL, New London
- 2 CO, USNUOS, Newport
- 1 CO, USNATC, Patuxent River
- 1 Supt, USNAVPGSCOL, Monterey
- 1 Dir, Marine Physical Lab, USNEL, San Diego
- 1 Chrm, Def Sci Board
- 1 CDR, W-PADEVCECEN
- 2 CDR, ASTIA
- 1 CG, Aberdeen PG
- 2 CG, ENGRESDEVLAB
- 1 Dir, NASA
- 3 Dir, Langley Res Ctr, NASA
- 2 Dir, Lewis Res Ctr, NASA
- 2 Dir, Ames Res Ctr, NASA
- 1 Dir, USAEC, Oak Ridge
- 2 Dir, Natl, BuStands
- 2 Hydro Lab, CIT, Pasadena
- 1 Dir, Inst of Engin Res, Univ of Calif, Berkeley
- 2 Dir, Iowa Inst of Hydraul Res, Univ of Iowa, Iowa City
- 2 Dir, Inst for Fluid Dyn & Appl Math, Univ of Maryland
- 2 Dir, Dept NAME, Univ of Michigan, Ann Arbor
- 2 Dir, DL, SIT, Hoboken
- 1 Dir, Jet Propul Lab CIT, Pasadena

Copies

- 1 Dir, Def Res Lab, Univ of Texas, Austin
- 1 Dir, St Anthony Falls Hydraul Lab, Univ of Minn, Minneapolis
- 2 Dir, ORL, Penn State
- 1 Dir, Midwest Res Inst, Kansas City
- 1 Dir, Robinson Model Basin, Webb Inst of Nav Arch, Glen Cove
- 2 Dept NAME, MIT, Cambridge
 - 1 Prof N. Abkowitz
- 2 SUPSHIP, Groton
 - 1 Electric Boat Div
- 2 NNS & DD Co
 - 1 Asst Nav Arch
 - 1 Dir, Hydraul Lab
- 1 Editor, Aero Engin Rev, New York
- 1 Editor, Appl Mech Rev, SW Res Inst, San Antonio
- 1 Editor, Bibliography of Tech Reports, Off of Tech Serv, Dept Comm
- 1 Editor, Engin Index, New York
- 2 Tech Lib, Douglas Aircraft Co, Inc, EL Segundo
 - 1 Mr. A.M.O. Smith
- 2 Tech Lib, North Amer Aviation, Inc, Downey
 - 1 Dr. E.R. van Driest
- 1 Dir, Dept of Engineering Sci, Univ of Notre Dame
- 2 Dean, School of Engineering & Arch, Catholic Univ of Amer
- 2 Dean, College of Engineering, Univ of Calif
 - 1 Dr. H.B. Nottage
- 2 Dir, Aero Res Lab, Melbourne, Australia
- 1 Dir, Inst of Aerophysics, Univ of Toronto, Toronto, Canada
- 3 NPL, Teddington, England
 - 1 Aero Div
 - 2 Ship Div
- 1 Head, Aero Dept, Royal Aircraft Estab, Farnborough, Hants, England
- 1 Dr. S.L. Smith, Dir, BSRA, London, England
 - 1 H. Lackenby
- 1 Dir, Bassin d'Essais des Carènes 6, Paris, France
- 1 Dir, Societe Grenbloise d'Etudes et d'Applications Hydrauliques, Grenoble, (Isere) France
- 1 Office, Natl d'Etudes et de Recherches Aeronautiques 3, Paris, France
- 1 Dr. J. Dieudonne, Dir, Gen Naval Constr Res Inst, Paris, France
- 2 ONERA, Serv des Relations Exterieures et de la Documentation, Chatillon-sous-Bagneux (Seine), France
- 1 Prof Dr. H. Schlichting, Institut fur Stromungs, Technische Hochschule, Braunschweig, Germany
- 1 Gen Ing u. Pugliese, Pres, Istituto Naz per Studi ed Esp di Arch Nav, Rome, Italy
- 1 Dir, Laboratorium Voor Aero-En Hydrodynamica, Delft, Netherlands

Copies

- 1 Dr. M. Lopez Acevedo, Dir, Canal de Experiencias Hidrodinamicas, Madrid, Spain
- 1 Dir, Nederland Scheepsbouwkundig Proefstation, Wageningen, Holland
- 1 Dr. Hans Edstrand, Dir, Statens Skeppsprovninganstalt, Goteborg, Sweden
- 1 Dir, Library of Chalmers Univ of Tech, Botenborg, Sweden
- 2 Dir, Institut fur Schiffbau der Universitat Hamburg, Hamburg, Germany
 - 1 Dr. K. Wiegardt
- 1 Dr. H.W. Lerbs, Dir, Hamburg Model Basin, Hamburg, Germany
- 1 Dir, ARL, Teddington, England
- 2 Dean College of Engineering, Seol Natl Univ, Seol, Korea
 - 1 Prof Cheung Hun Kim, Dept of Nav Arch

MIT LIBRARIES

DUPL



3 9080 02754 3393

